

TSUNAMI WAVE PROPAGATION ALONG WAVEGUIDES

Andrei G. Marchuk

*Institute of Computational Mathematics and Mathematical Geophysics
Siberian Division Russian Academy of Sciences, 630090, Novosibirsk, RUSSIA*
mag@omzg.sccc.ru

ABSTRACT

This is a study of tsunami wave propagation along the waveguide on a bottom ridge with flat sloping sides, using the wave rays method. During propagation along such waveguide the single tsunami wave transforms into a wave train. The expression for the guiding velocities of the fastest and slowest signals is defined. The tsunami wave behavior above the ocean bottom ridges, which have various model profiles, is investigated numerically with the help of finite difference method. Results of numerical experiments show that the highest waves are detected above a ridge with flat sloping sides. Examples of tsunami propagation along bottom ridges of the Pacific Ocean are presented.

Science of Tsunami Hazards, Vol. 28, No. 5, page 283 (2009)

INTRODUCTION

The qualitative theory of waveguides in a media with varying optical density (velocity of signals or waves in it) as well as the concept of waveguides with total reflecting boundaries have been discussed in the literature (Brekhovskikh [1]). Based on such previous work, the present study introduces the concept of waveguides in an application related to the tsunami problem. In a two-dimensional space the velocity of wave disturbance propagation caused by a sudden disturbance is constant and represented by v_0 . In a linear regime it decreases monotonically and reaches a minimum value along the axis. This linear axis where wave propagation velocity is less than v_0 is named “waveguide”. If a wave origin source is initially located on such waveguide, a portion of the energy will be captured and the waves will propagate along its length for a long time - more than likely to the very end of it. The present study examines the linearly varying but increasing wave propagation velocity along the axis of the waveguide. The postulated waveguides look like bottom ridges with flat sloping sides. A plane wave on the mean water surface is assumed to be the origin source and the initial propagation direction of the wave's front is along the waveguide's axis. The present study develops the quantitative theory of the wave propagating process for waveguides of this type.

Determination of wave rays above the sloping bottom.

Wave rays, widely used in wave kinematic investigations, can be determined as curves, orthogonally directing the propagating wave front at every moment of time. In other words they are the trajectories of wave front-line points during wave propagation. In an area of constant depth all such rays have the form of straight lines. Based on long-wave theory the propagation velocity for tsunami waves depends only on water depth and is defined by Lagrange's formula

$$c = \sqrt{gH}. \quad (1)$$

Wave-rays can be defined as the quickest routes of a perturbation's propagation. Wave rays are the orthogonal lines of energy directivity along a tsunami's wave front. In ocean areas of variable depths, the wave rays do not usually follow straight line paths. Thus, in general, the problem of tsunami travel-time determination from one point to another, cannot be easily and accurately determined. The integral which describes the time required for a perturbation (tsunami wave) to move between points A and C, in the XOY plane is given by:

$$T = \int_{\gamma} \frac{dS}{c(x, y)}, \quad (2)$$

where dS is an element of the γ curve, connecting the points A and C (Fig. 1).

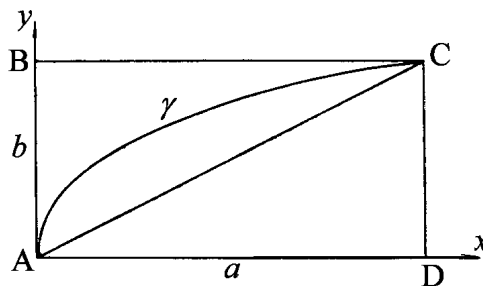


Fig. 1. Diagram of problem of determining the tsunami travel-time from the source to the point on the shore line (the wave-ray definition problem)

We must now determine the curve γ which minimizes the integral (2). After the trace determination it is easy to calculate the required tsunami travel-time from point **A** to point **C**. One of the possible ways in determining a wave front's ray trace is by numerical solution of the Cauchy problem and the use of governing differential equations. In the case of simple distribution of water depth $H(x, y)$ one can find analytically the $y(x)$ curve of interest, and obtain the explicit formula for the time required for tsunami wave propagation. We can also proceed with this procedure for a sloping ocean floor. The derived solution can explain some of the effects which take place during the tsunami wave propagation in the near shore zone.

Let us now consider the following problem: we have a rectangular section **ABCD** of the ocean, near the shore (Fig. 1). The sides are a and b long. The point **A**, which is on the shore-line, we shall assume to be the zero point of the Descartes coordinate system XOY . Let us also assume that the depth will increase linearly from **AD** side towards **BC** side, as per the following rule

$$H(x, y) = \operatorname{tg}(\alpha) \cdot y, \quad H(B) = H(C) = a \cdot \operatorname{tg}(\alpha) = H_0, \quad (3)$$

$$H(A) = H(D) = 0,$$

where α is the bottom inclination angle with respect to the horizon.

Let us also assume that at the point **C** at the moment in time $t=0$, a tsunamigenic earthquake took place. The problem is to determine the time interval at which the wave will reach point **A**. The earthquake generated tsunami wave will propagate in all directions but there is a certain optimal trajectory γ , along which the perturbation will reach point **A** at the shortest time. This is precisely the trajectory which we determine in order to find the time required for the propagation of this tsunami wave along this trajectory. As already stated, because of the relationship between frontal wave propagation rate and depth (1), the optimal trajectory is not a straight line, connecting **C** and **A** points. In fact, it will be a curve, which lies to the right of the **AC** diagonal line, in moving from the point **C** to the point **A** - in other words, in the area of greater depth (see Figure 1). Thus, the time of the wave movement along the γ curve is given by:

$$T = \int_{\gamma} \frac{d\gamma}{\sqrt{gH}} = \int_{\gamma} \frac{\sqrt{dx^2 + dy^2}}{\sqrt{g \cdot y \cdot \operatorname{tg}(\alpha)}} = \int_{\gamma} \frac{\sqrt{1 + (y')^2}}{\sqrt{g \cdot y \cdot \operatorname{tg}(\alpha)}} dx = \frac{1}{\sqrt{g \cdot \operatorname{tg}(\alpha)}} \int_{\gamma} \frac{\sqrt{1 + (y')^2}}{\sqrt{y}} dx, \quad (4)$$

where $y' = dy/dx$. To solve the tsunami travel-time minimization problem it is necessary to determine the minimum of the integral (4) along all possible curves $y(x)$, connecting the points **C** and **A**.

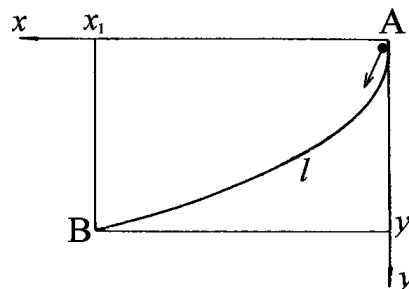


Fig. 2. Diagram of the brachistochrone problem

Let us now make use of the mechanical analogy, assuming that there are two points $\mathbf{A}(0,0)$ and $\mathbf{B}(a,b)$ located on the vertical plane XOY . In this case, the OY axis is directed downward and coincides with the force of gravity (Figure 2).

It is necessary to find such curve, connecting points \mathbf{A} and \mathbf{B} , along which a heavy ball, by rolling down under the force of gravity, from point \mathbf{A} , will reach point \mathbf{B} in the shortest time. Such ball starts its movement from a state of rest (brachistochrone problem). Because of the energy conservation law, the ball modulus of velocity can be expressed by the following formula:

$$v = \sqrt{2gy}. \quad (5)$$

It can be easily seen that in this case the time required for this ball to move along the curve l , connecting points \mathbf{A} and \mathbf{B} , may be expressed as follows:

$$T_1 = \int_l \frac{\sqrt{1+(y')^2}}{\sqrt{2gy}} dx = \frac{1}{\sqrt{2g}} \int_l \frac{\sqrt{1+(y')^2}}{\sqrt{y}} dx. \quad (6)$$

By comparing formulas (4) and (6) one can easily see that the time T and T_1 , differ in terms of a constant factor

$$T_1 = \sqrt{\frac{tg(\alpha)}{2}} T.$$

In other words, we are to minimize the same integral as in the case, related to the tsunami wave propagation. The problem of the rolling ball is a classical problem of mechanics, which is solved by using the variation calculus method (Elsgol'ts [2]). Let us now express the ball's travel time (6) from the point $\mathbf{A}(0,0)$ to point $\mathbf{B}(x_l, y_l)$ as a functional of the curve shape $y(x)$

$$F(y(x)) = T(y(x)) = \frac{1}{\sqrt{2g}} \int_0^{x_l} \frac{\sqrt{1+(y')^2}}{\sqrt{y}} dx, \quad y(0)=0, \quad y_l=(y(x_l)). \quad (7)$$

The integrand of this functional does not explicitly contain the x coordinate. So, the condition of minimum of this functional [2] is expressed as

$$F - y'F_y = C,$$

where C is a constant. For this particular case (a rolling ball)

$$\frac{\sqrt{1+(y')^2}}{\sqrt{y}} - \frac{(y')^2}{\sqrt{y(1+(y')^2)}} = C. \quad (8)$$

After simplifying we have

$$\frac{1}{\sqrt{y(1+(y')^2)}} = C,$$

$$y(1+(y')^2) = \frac{1}{C^2} = C_1. \quad (9)$$

After introducing a new parameter t , which is defined as $y' = \text{ctg}(t)$, formula (9) can be transformed to

$$y = \frac{C_1}{1 + \text{ctg}^2 t} = C_1 \sin^2 t = \frac{C_1}{2}(1 - \cos(2t)),$$

$$dx = \frac{dy}{y'} = \frac{2C_1 \sin(t)\cos(t)dt}{\text{ctg}(t)} = 2C_1 \sin^2(t)dt = C_1(1 - \cos(2t))dt,$$

$$x = C_1 \left(t - \frac{\sin(2t)}{2} \right) + C_2 = \frac{C_1}{2}(2t - \sin(2t)) + C_2.$$

Finally we have the parametric form of the curve, that provide the minimum of the ball's moving time

$$x - C_2 = \frac{C_1}{2}(2t - \sin(2t)), \quad y = \frac{C_1}{2}(1 - \cos(2t)),$$

Where $t=0$ at the starting point $A(0,0)$. The constant C_2 is equal to zero, because the curve begins from the zero point $A(0,0)$. After substitution $2t=t_1$ we will have equations of the cycloid (trajectory of the point on a circle during its rolling over horizontal line $y=0$) in parametric form:

$$x = \frac{C_1}{2}(t_1 - \sin(t_1)), \quad y = \frac{C_1}{2}(1 - \cos(t_1)),$$

where $C_1/2$ is the radius of the rolling circle, which can be determined on the basis of the cycloid passage through the point $B(x_1, y_1)$ (the second point is the starting point of the coordinates). So, the solution of this problem, in other words, the optimal trajectory, would be a cycloid, which in its parametric form will be written as follows

$$\begin{aligned} x &= C(t - \sin(t)), \\ y &= C(1 - \cos(t)). \end{aligned} \tag{10}$$

At the point (x_1, y_1) , the t parameter value will be as follows

$$t = t^* = \arccos\left(1 - \frac{y_1}{C(x_1, y_1)}\right).$$

Further, the time of the movement of the ball, from the point A to point B along the cycloid may be expressed by the following integral:

$$\begin{aligned} T_1 &= \int_0^{y_1} \frac{\sqrt{1 + (y')^2}}{\sqrt{2gy}} dx = \frac{1}{\sqrt{2g}} \int_0^{t^*} \frac{\sqrt{1 + \frac{\sin^2(t)}{(1 - \cos(t))^2}}}{\sqrt{c_1(1 - \cos(t))}} (1 - \cos(t)) dt = \\ &= \frac{1}{\sqrt{2g}} \int_0^{t^*} \sqrt{2C} dt = \frac{\sqrt{2C}}{\sqrt{2g}} t^*. \end{aligned} \tag{11}$$

Let's go back to the tsunami problem. If the tsunami wave propagates across the area with a sloping bottom, then instead of velocity $\sqrt{2gy}$ in formulas (6) and (11), there will be the value $\sqrt{g \cdot \text{tg}(\alpha) \cdot y}$. Consequently, for the tsunami travel-time between points (a,b) and $(0,0)$ the following expression will be valid:

$$T = \frac{\sqrt{2C}}{\sqrt{g \cdot \text{tg}(\alpha)}} \cdot \arccos\left(1 - \frac{b}{C}\right), \quad (12)$$

where, as already mentioned, C is a constant, which is defined on the basis of the cycloid passage through the point (a, b) .

Investigation of waveguides using wave rays

Let us now study the process of tsunami wave propagation above the submerged ridge with flat sloping sides (Fig. 3). Let us also use the limited bottom slope with the fully reflecting boundary for such an investigation (Fig. 4). The 2D view on this rectangular water area with sloping bottom is presented in Figure 5. In the Cartesian coordinate system the depth is linearly increasing from zero on the **OX** axis ($y = 0$) by formula $H = y \cdot \text{tg}(\alpha)$, where α is inclination angle of the bottom slope.

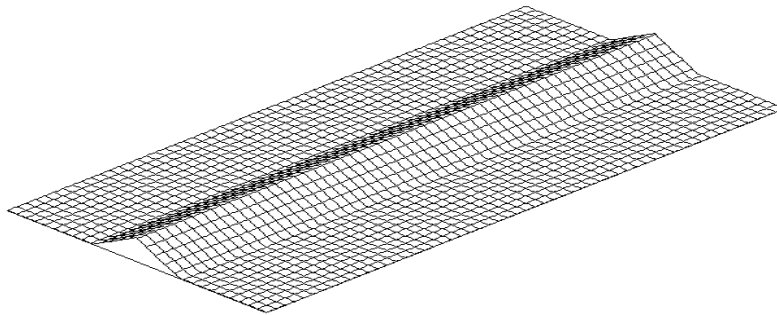


Fig. 3. A bottom relief simulating underwater mountain ridge

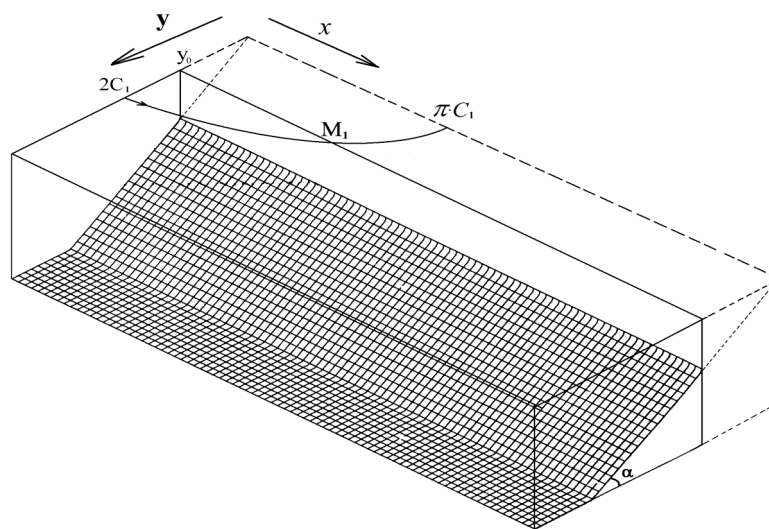


Fig. 4. 3D-view on a wave ray trajectory above the bottom slope

If from a point $(0, 2C_1)$ the wave ray started in parallel to OX axis direction, it will look like a segment of cycloid having radius C_1 (the radius of the rolling circle), and its trajectory can be described by equations

$$\begin{aligned} x &= C_1(t - \sin(t) - \pi), \\ y &= C_1(1 - \cos(t)), \quad t \in (\pi, 2\pi). \end{aligned} \quad (13)$$

The ray will reach an axis OX in a point $(x_2, 0)$ (Fig. 5), where $x_2 = \pi \cdot C_1$. If the plane of bottom has the same declination, but the decreasing of depth stops on the line $y = y_0$ where the reflecting boundary is installed. The ray, after arriving to the point M_1 that is situated on the distance y_0 from the OX axis, will reflect from the line $y = y_0$. After reflection the wave ray will go to the point M_2 along the new cycloid with the same radius (see fig. 5). The condition of reflection of a wave ray on a line $y = y_0$, is caused by symmetry of a picture relatively to the axis $y = y_0$ that is true for symmetrical waveguides. The strip region $y_0 < y < 2C_1$ in Figure 5 simulates the sloping side of the bottom ridge (waveguide).

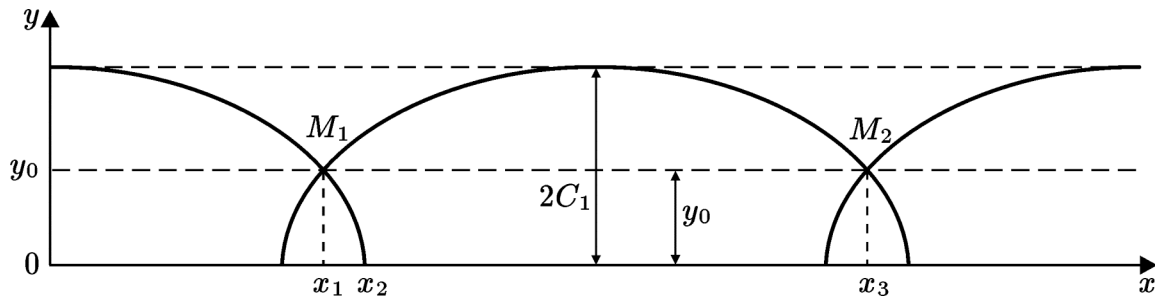


Fig. 5. Trajectory parameters during the wave ray motion above the bottom slope

Let us now determine the length of a step of this truncated cycloid, and also the wave travel time along it. As length of a step of a full cycloid is expressed as $L = 2\pi C_1$, the length of a step of a truncated cycloid (Fig. 5) will be expressed as follows

$$L_1 = x_3 - x_1 = L - 2(x_2 - x_1). \quad (14)$$

The value $(x_2 - x_1)$ easily can be define from the equation of a cycloid (13)

$$L_1 = 2\pi C_1 - 2C_1 \left(\arccos\left(1 - \frac{y_0}{C_1}\right) - \sin\left(\arccos\left(1 - \frac{y_0}{C_1}\right)\right) \right). \quad (15)$$

The wave travel-time along this cycloid can be written as follows

$$T = \frac{2\sqrt{2C_1}}{\sqrt{g \cdot \operatorname{tg}(\alpha)}} \left(\pi - \arccos\left(1 - \frac{y_0}{C_1}\right) \right). \quad (16)$$

Here α is the inclination angle of the bottom plane to horizon, C_1 - radius of a cycloid. If maximum depth H_0 outside of the waveguide and minimum depth on a ridge H_1 is given, then

$$C_1 = \frac{H_0}{2\text{tg}(\alpha)}, \quad y_0 = \frac{H_1}{\text{tg}(\alpha)}, \quad l = (2C_1 - y_0), \quad (17)$$

where l is a half-width of the waveguide, if the waveguide is twice wider ($l_1 = 2l$), but the depth variation remains the same. In this case the declination of bottom $\text{tg}(\beta)$ will be reduced down to half of the former value and will become

$$\text{tg}(\beta) = \frac{\text{tg}(\alpha)}{2}.$$

Due to this, the radius of cycloid appropriate to "lateral" rays, reaching the edges (borders) of the waveguide, will be doubled, $C_2 = 2C_1$. The value y_2 also will increase ($y_2 = 2y_0$). The wave travel-time from the axis up to the edges of the waveguide along the new cycloid will be written as

$$T_2 = \frac{2\sqrt{4C_1}}{\sqrt{(g \cdot \text{tg}(\alpha))/2}} \left(\pi - \arccos\left(1 - \frac{2y_0}{2C_1}\right) \right) = 2T_1. \quad (18)$$

The length of the cycloid step will be increased also by 2 times. Therefore, the average speed along the waveguide of the signals which propagate along "extreme" rays does not depend on the waveguide width and is determined only by the difference of depths H_0 and H_1 .

Let us now investigate the propagation velocity of different segments of the wave front along the waveguide depending on their initial distance from the axis. In Fig. 6 the trajectories of the wave rays, which are started at distance $2y_1$ and y_1 away from the axis of the waveguide and the wave ray, traveling along the axis, are shown.

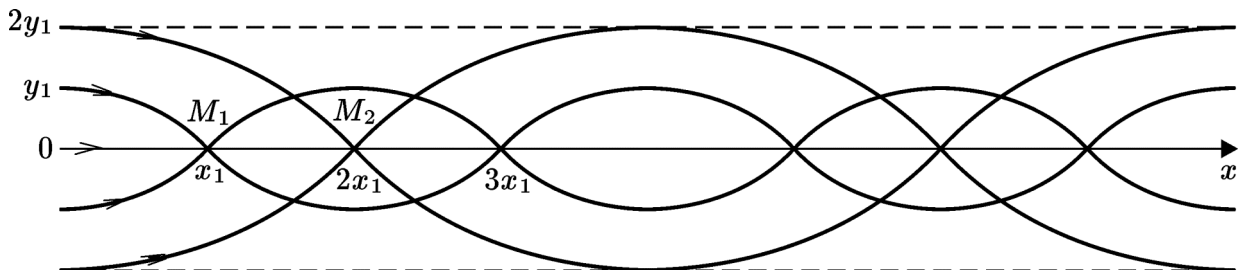


Fig. 6. Wave rays in the symmetric waveguide

Let l be the half-width of the waveguide, α - angle of inclination of the planes of bottom, H_0 - depth outside of the waveguide. The basic values we need for calculation are defined as

$$H_1 = H_0 - l \cdot \text{tg}(\alpha), \quad y_0 = H_1 / \text{tg}(\alpha), \quad (19)$$

where H_1 is the depth above a ridge. The value C_1 (radius of cycloid) depends on initial distance y_1 from an axis of the waveguide to a wave-ray starting point

$$C_1 = (y_0 + y_1) / 2, \quad 0 \leq y_1 \leq l.$$

Using expressions (15) and (16) the ratio between an average wave velocity V along the waveguide and value y_1 (or C_1) can be defined

$$V = \frac{L}{T} = \frac{2\pi C_1 - 2C_1 \left(\arccos\left(1 - \frac{y_0}{C_1}\right) - \sin\left(\arccos\left(1 - \frac{y_0}{C_1}\right)\right) \right)}{\frac{2\sqrt{2C_1}}{\sqrt{g \cdot tg(\alpha)}} \left(\pi - \arccos\left(1 - \frac{y_0}{C_1}\right) \right)}, \quad (20)$$

where the values C_1 and y_0 are determined by formulas (17). The velocity of an appropriate wave motion along the waveguide depends on value C_1 (or y_1) and it is as less, as closer the initial wave ray to the axis. Let's find a speed limit V , when parameter y_1 is going to y_0 . Let y_0 differs from y_1 by a small value ε .

$$y_0 = y_1 \left(1 - \frac{\varepsilon}{2}\right) = 2C_1 - \varepsilon C_1.$$

Then, keeping in the formula (20) members of the least order by ε , we arrive at

$$V \approx \frac{2C_1 \left(\pi - (\pi - \sqrt{\varepsilon}) + \sqrt{\varepsilon} \right)}{\frac{2\sqrt{2C_1}}{\sqrt{g \cdot tg(\alpha)}} \left(\pi - (\pi - \sqrt{\varepsilon}) \right)} = \sqrt{2gC_1 \cdot tg(\alpha)}, \quad (21)$$

that corresponds to a disturbances propagation velocity along the axis of waveguide calculated by Lagrange formula $V = \sqrt{gH_1}$, which is applied to the top of ridge

$$C_1 = \frac{H_1}{2tg(\alpha)}.$$

Thus, each waveguide (not only with flat bottom planes) has a specific dispersion, which is discovered in expansion of the initial plane wave along the waveguide during its propagation. Finally the initial single wave will transform into a wave "train". This dispersion ability of each waveguide can be measured by value $q = V_{\max} / V_{\min}$, where V_{\max} is the running speed of fastest rays along the waveguide and V_{\min} the running speed of the slowest wave ray that coincides with the axis of waveguide.

Let us subsequently study the problem of wave energy focusing by the waveguide. Above a flat bottom the amplitude of a circle tsunami wave is decreasing due to cylindrical divergence proportionally $R^{-1/2}$, where R - distance from a source. Getting into the waveguide, the wave amplitude is not more decreased due to cylindrical divergence. However from this moment the wave energy disperses by stretching the initial single wave along the axis of waveguide, that also causing reduction of amplitude. If the rate of amplitude loss due to wave dispersion along the waveguide is less than the possible amplitude loss due to cylindrical stretching of the front, in this case a waveguide has focusing properties. Mathematically it can be written as follows:

$$(V_{\max} - V_{\min}) \cdot T < \frac{2\pi}{K} R^{1/2}. \quad (22)$$

Here T - time of motion of a waveguide waves, K - value indicating, what part of circle front of an incident wave has got in the waveguide, R - distance from the wave source up to a position of front in the waveguide after time period T . Thus, not every waveguide causes a focusing effect. It is the broader waveguides with small depths differences ($H_0 - H_1$) that have the greatest focusing ability. The most favorable situation for focusing arises when the tsunami wave source is situated above the waveguide.

Let us now remark about asymmetrical waveguides, where the declination of flat bottom is various for different sides from the ridge. Let the declination of one side be 2 times greater, than the other. The depth outside the waveguide is equal to H_0 and on the ridge (axis) - H_1 . Let us consider trajectories of "lateral" rays, which reach the borders of the waveguide. In the initial moment they lay out on distances y_2 and $y_1 = 2y_2$ on both sides from the axis of waveguide (Fig. 7).

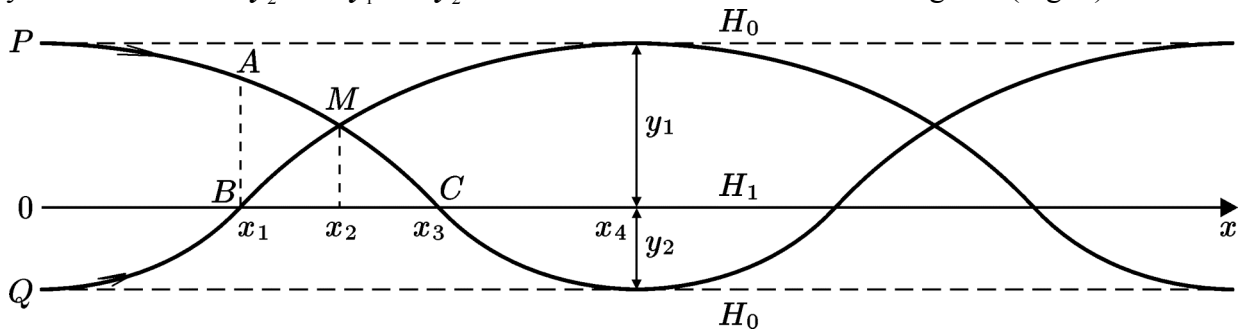


Fig. 7. Trajectories of "lateral" rays in an asymmetric waveguide

As previously-stated, the radius of cycloids, along which wave rays propagate above the more flat side, is twice greater than the radius of both of the rays under consideration, when propagating above the other side which has greater inclination. As seen in Figure 7, both rays have identical-length paths before reaching cross-section $x = x_4$, and each consisting of two cycloid pieces. Thus, on the cross-section $x = x_4$ the rays arrive simultaneously. The cross point M of these "lateral" wave rays is not located on the axis of the waveguide Ox . In spite of point M being a cross point of wave rays (a caustic), the noticeable increase of a wave amplitude in it is not detected, because the rays do not come to this point simultaneously. Let us show this as $y_1 = 2y_2$, then $x_3 = 2x_1$. The wave travel-time along the "large" cycloid is more than twice as that along the "small" (time T_0). Taking into account that the travel-time along the curve PC is equal $2T_0$, the travel-time along the curve PA will be less than T_0 , because the length of PA is less than the length of AM . Furthermore, along PA the depths are greater. Moreover, the wave travel-time along the curve AM will be less, than along BM , because the length of AM is less than the length of BM , and the curve AM is located along greater depth. Thus, the wave reaching point M along the curve PM will arrive much earlier, than that along the curve QM . Let us also estimate the propagating velocity of "lateral" rays along the waveguide, i.e. V_{max} . These rays will arrive simultaneously at the cross-section $x = x_4$ and their travel-time will be $3T_0$. Therefore the average wave speed along the waveguide is expressed as x_1 / T_0 , that is equal to V_{max} for symmetrical waveguides with the same depths on a ridge and the outside of the waveguide. Therefore the statement about the independence of the wave propagating velocity along the waveguide from its width is correct also for asymmetrical waveguides.

Now - as mentioned above - let us consider a ratio of tsunami amplitudes in the wave train that arises as a result of dispersion. Using relation (20), we find some values of propagating velocity V along the ridge for wave rays, which are disposed at different distances from the axis of

the waveguide. The derived values of propagating velocity V for that waveguide, suggest that the relation V from y_1 is rather close to linear, but for rays initially disposed closer to the waveguide edge, the varying rate of V depending on distance y_1 is lower than for rays initially located closer to the axis of the waveguide. Thus, the dispersion of the waveguide impacts a little bit stronger on the slowly moving part of a “wave train” and, consequently, the leading waves from a dispersing signal have slightly greater amplitude, than in the “tail” of the same “wave train”.

In the case when on an entrance of the waveguide is perpendicular to its axis there are not one, but two consecutive waves. Let us assume that between positive maximums of these waves the initial distance is equal to 2λ . Then above the waveguide the waves will transform into “wave trains”. The “leading” part of the second wave can reach the “tail” of the first wave and that will cause amplification of wave amplitude above an axis of the waveguide. It is possible to determine the causing conditions. Assuming that the initial distance between wave maximums in the waveguide is equal 2λ . Let the maximum and minimum wave rays propagating velocities of the waveguide be equal to V_{\max} and V_{\min} . The distance between the “tail” of the first wave and “leading” part of the second wave will be expressed as

$$l = V_{\min} \cdot T + 2\lambda - V_{\max} \cdot T, \quad (23)$$

where T is the propagating time. Therefore, in time T_0 , when l will become zero, the dispersed signals from both waves will be imposed on each other, and that will cause the amplification of oscillations near the axis of waveguide on the distance $T_0 \cdot V_{\min}$ from its beginning. Hereinafter if there is imposing (superposition) of signal, the oscillation frequency in the waveguide fades out, as the process of waveguide dispersion promotes easing (attenuation) of both wave trains. Thus, the maximum level fluctuation in the waveguide is watched apart $T_0 \cdot V_{\min}$ from a beginning of the waveguide. The time period T_0 is determined by the characteristics of the waveguide

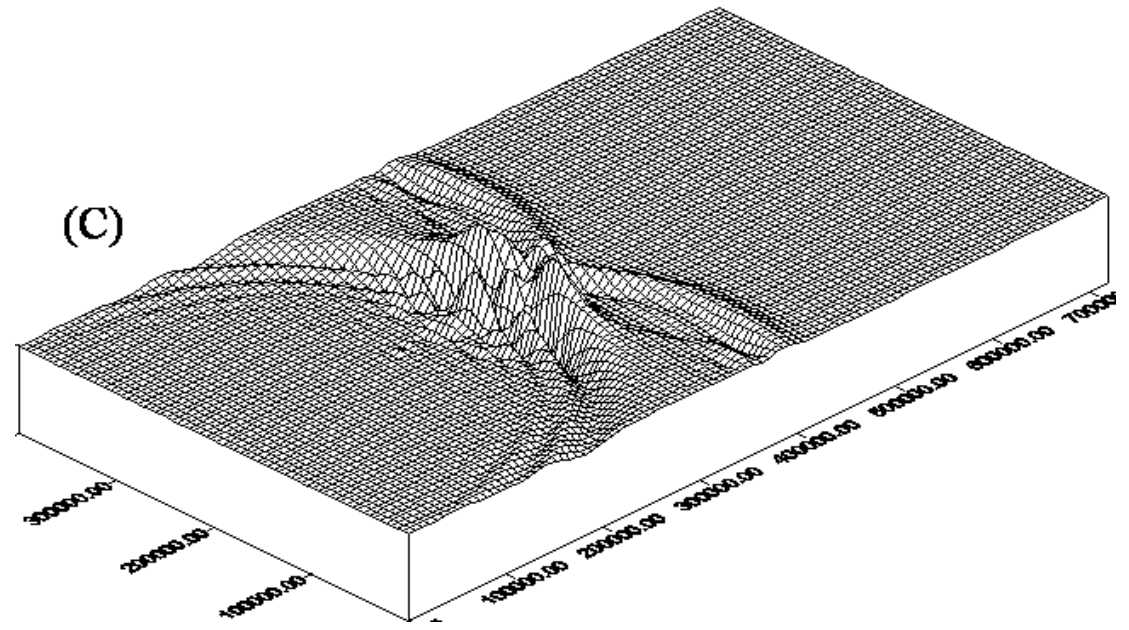
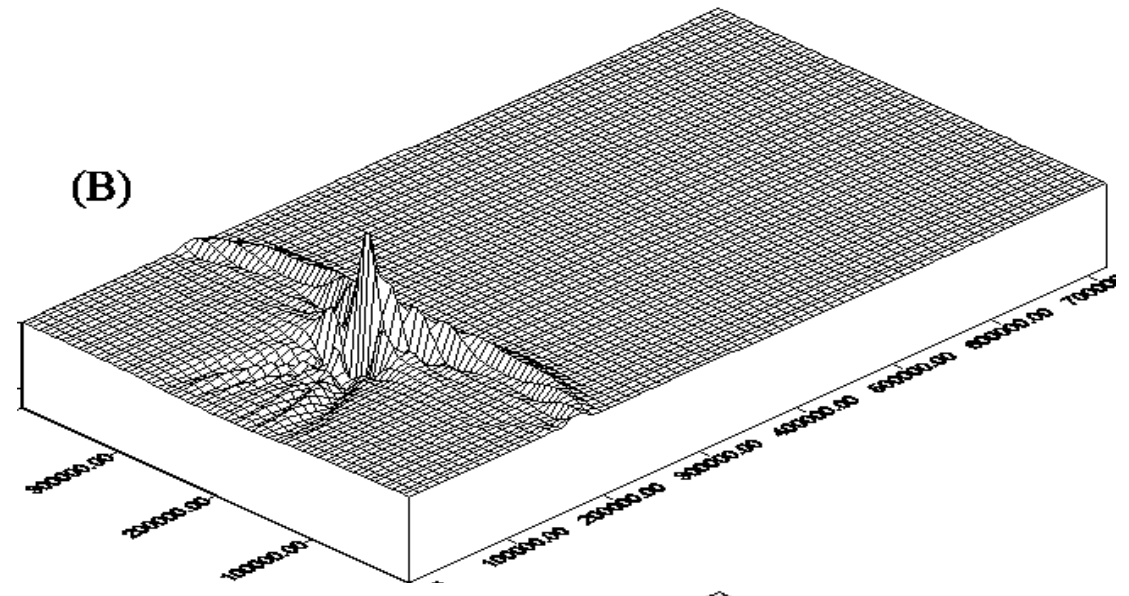
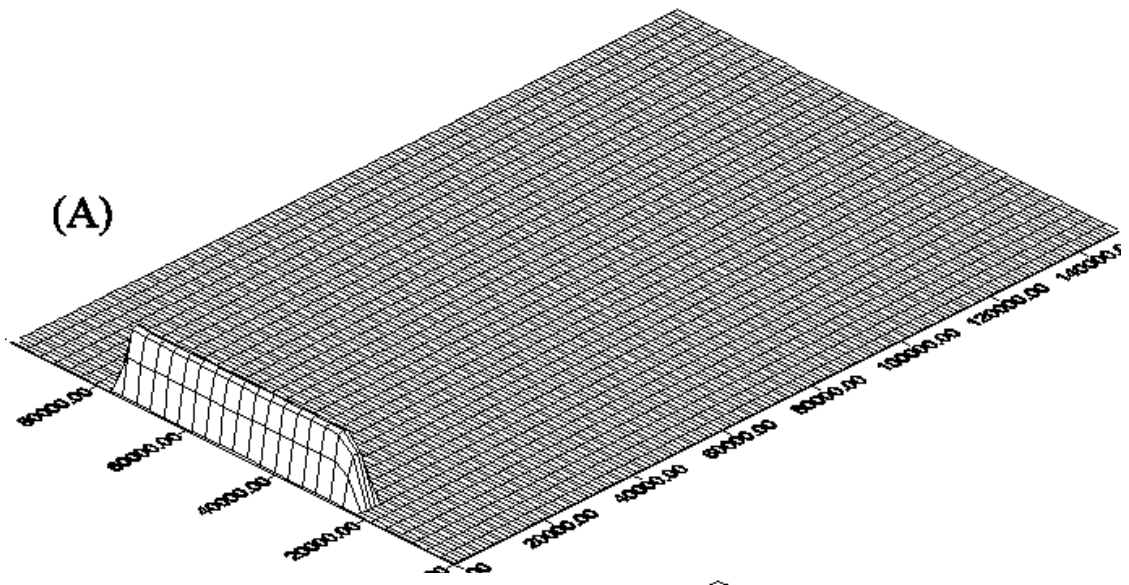
$$T_0 = \frac{2\lambda}{V_{\max} - V_{\min}}. \quad (24)$$

If the initial wave signals, propagating in the waveguide, have negative parts, then a picture of interaction of this waveguide waves will be more complicated.

Numerical experiments

To confirm the theoretical description of tsunami wave behavior in the waveguide of the indicated type, numerical modeling was carried out of tsunami wave propagation above underwater ridge, having a model relief as shown in Figure 3. A numerical algorithm based on variables splitting method (Titov [3]) was used for tsunami propagation modeling. The size of the computational area was 720 km x 400 km (720 x 400 grid-points), and the width of the waveguide was 200 km. The depth along an axis of the waveguide was equal to 500 m, and outside of the waveguide - 1,000 meters. The input tsunami was 4 meters high and was shaped as a long narrow rectangle (20 x 200 grid-points) with the profile, which is determined by the expression

$$\eta = 2 + 2 \sin\left(\frac{i\pi}{10} - \frac{\pi}{2}\right), \quad (i=1, \dots, 20). \quad (25)$$



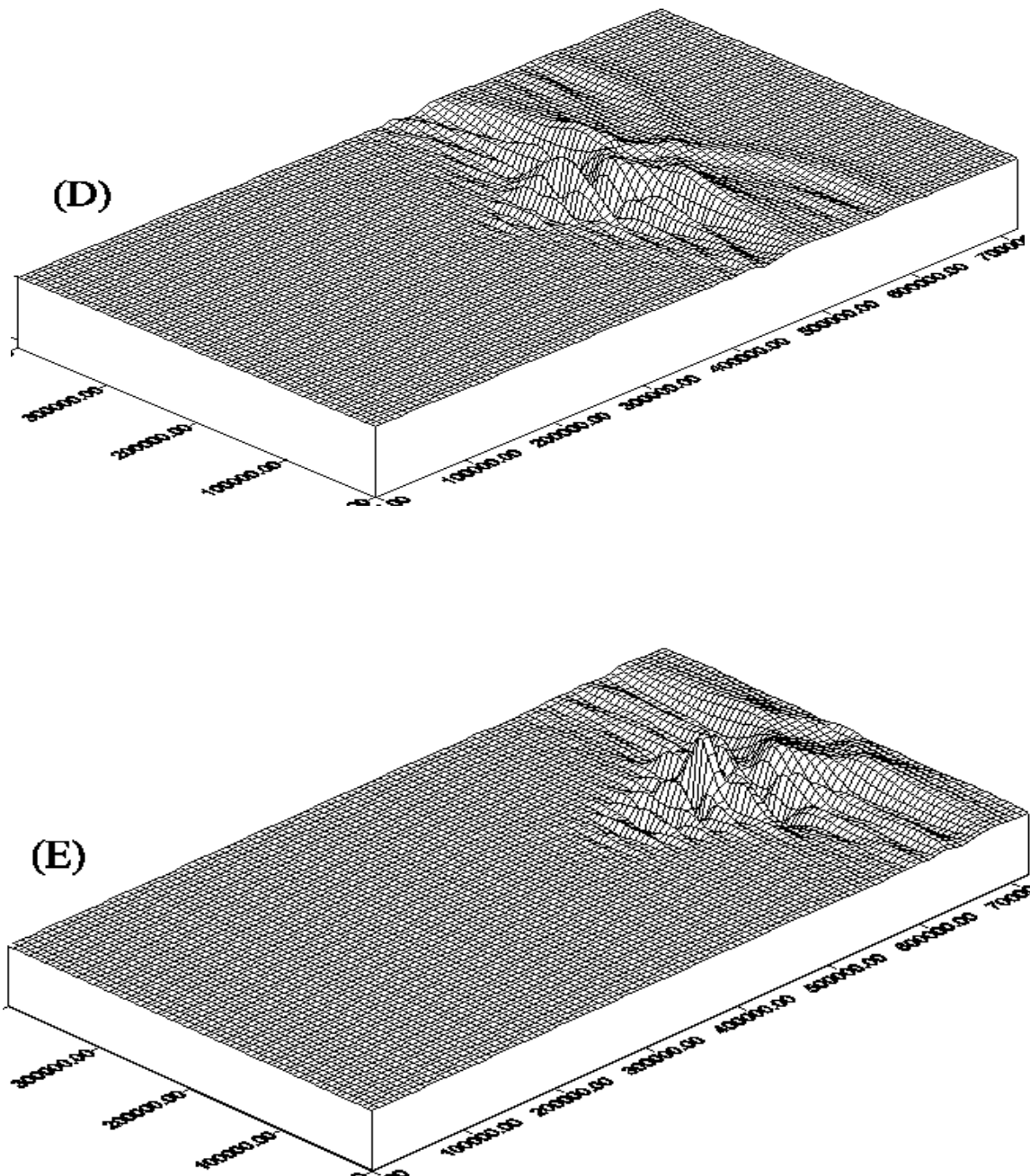


Fig 8A-8E. Water surface above the waveguide in various time moments

Figures 8A-8E show the ocean surface in different moments of wave propagation along the waveguide with flat sides (Fig. 3). The initial elevation of the water surface (fig. 8A) is forming a 2 meters high tsunami wave. The water surface at subsequent moments of time (2000 sec, 4000 sec, 8000 sec, 10000 sec) is shown in Fig. 8B-8E. As shown, that initial wave expands along the axis of waveguide and is transformed into a “wave train” with narrow front that completely confirms the theoretical results.

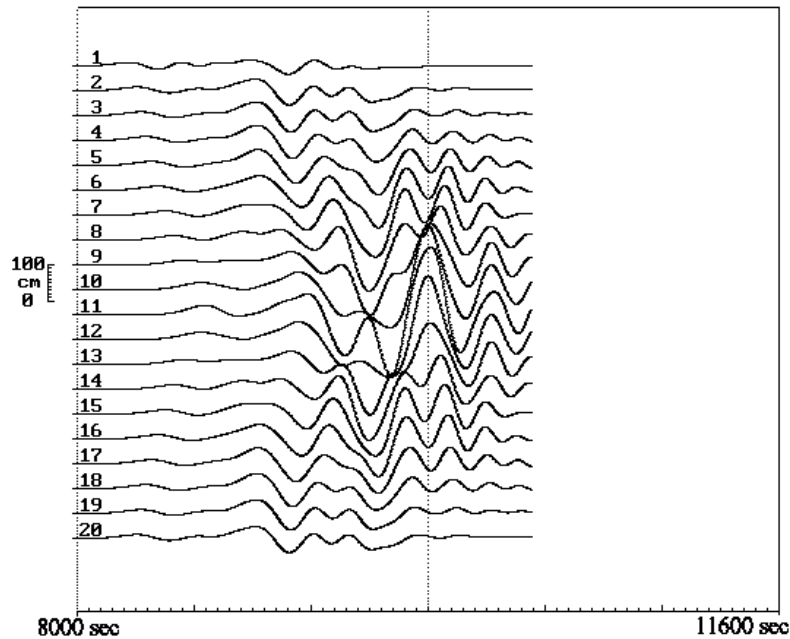


Fig. 9. Tsunami time series across the waveguide.

Figure 9 shows tsunami time series (marigrams) at a distance of 650 km from the tsunami source (the total length of the computational area being equal to 720 km). These marigrams correspond to 20 grid-points ($650, 100+10(j-1)$), which are located across of the computational area. Here $j=1 \dots 20$ is an index of time series (Fig. 9). Numerical results confirm the wave amplitude growth at the waveguide axis. Time series with index 11 (Fig. 9) was recorded just at the waveguide axis. The maximum tsunami wave height was detected here.

The profiles of water surface along the waveguide axis at the different time moments are shown in Figure 10. The Figure 11 presents free surface profiles along the same line ($j=200$) for the case of flat bottom (depth is equal to 1000 m) without any bottom ridge. In both computational experiments the initial 4 meters high source (25) generates the identical 2 meters high wave (top drawings in Figures 10 and 11).

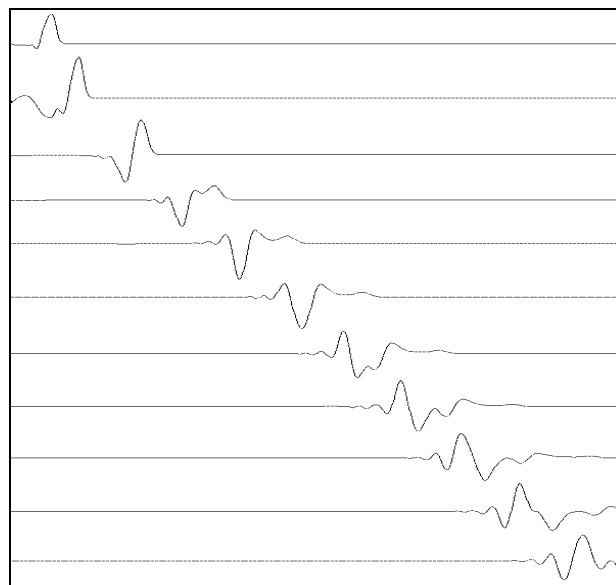


Fig. 10. Wave profile visualizations during tsunami propagation above the bottom ridge

As an example, let us estimate the average propagating velocities of fastest and slowest waves along this waveguide. For numerical computations the following parameters of the waveguide were used: $H_0=1000$ m, $H_1=500$ m. The fastest wave signal moves along the “lateral” wave ray having radius

$$C_1 = \frac{H_0}{2\text{tg}(\alpha)} = \frac{y_1}{2},$$

where H_0 is the depth outside bottom ridge. The other parameters are linked by formula

$$y_0 = y_1/2 = C_1.$$

Expression for the fastest wave propagation velocity (20) in this case will be written as

$$V = \frac{2C_1(\pi - \pi/2 + 1)}{2\sqrt{2C_1}(\pi - \pi/2)} = \frac{\sqrt{2C_1 \cdot g \cdot \text{tg}(\alpha)}}{2} \left(1 + \frac{2}{\pi}\right) = V_0 \frac{(1 + 2/\pi)}{\sqrt{2}} \approx 1.17 \cdot V_0.$$

Here $V_0 = \sqrt{gH_1} = \sqrt{gC_1 \cdot \text{tg}(\alpha)}$ is the slowest wave propagation speed (above the waveguide axis). This estimate is in good agreement with numerical results (Fig. 10).

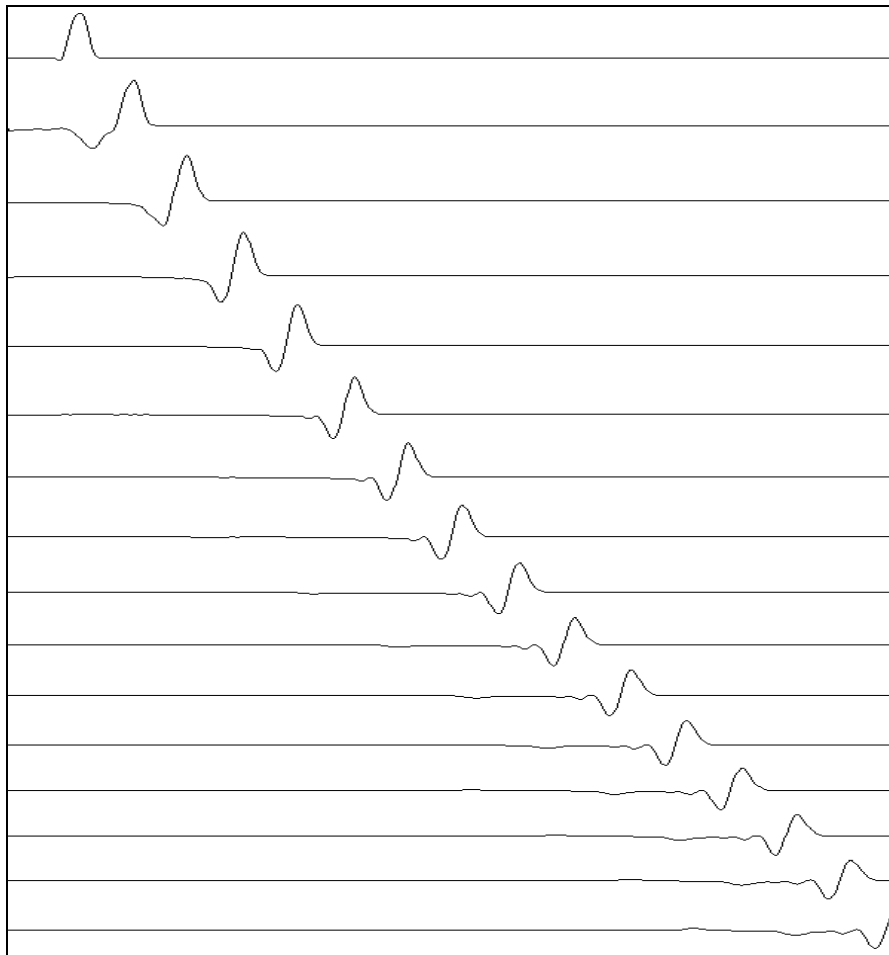


Fig. 11. Wave profile visualizations during tsunami propagation above the flat bottom

The comparison of wave amplitudes in the waveguide above the flat bottom indicates the significant amplitude growth above the axis (199 cm as compared to 85 cm without waveguide). In other words the amplitude of a tsunami wave which is propagating along this waveguide doesn't decrease during the first 3 hours of propagation.

A number of different ridge profiles were used in numerical computations. The profile of the bottom ridge was determined by the following formula

$$H(y) = H_1 + (H_0 - H_1) \frac{y}{y_0} - k \cdot \sin\left(\frac{\pi y}{y_0}\right), \quad (26)$$

where y is the distance from an axis, H_1 - the water depth on the axis, H_0 - the depth outside the waveguide and k is parameter, which varies from -150 to +150. When $k=0$ the ridge sides are flat. Waveguide sections for $k=-100$, $k=0$, $k=+50$, $k=+150$ (from the top to the bottom of the figure) are shown in Fig. 12.

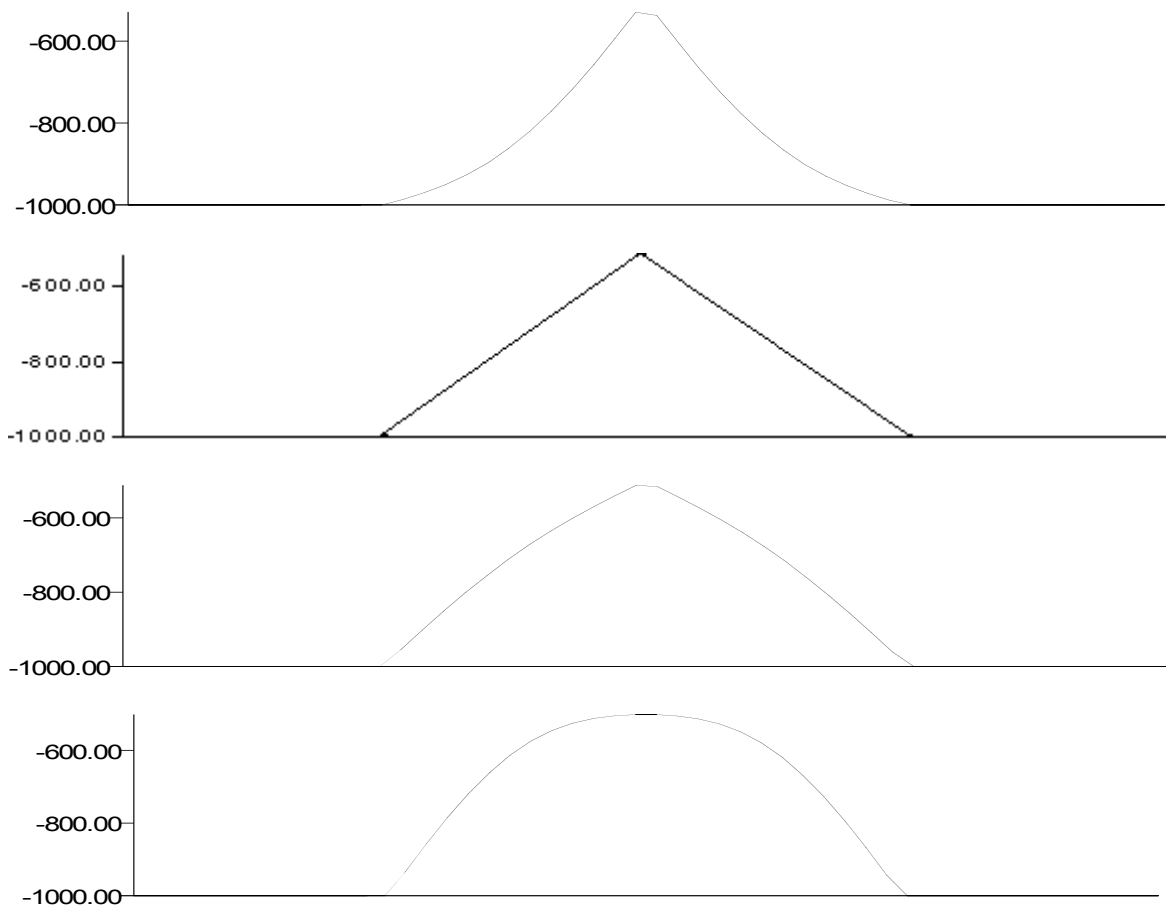


Fig 12. Profiles of the bottom ridge for different values of parameter k

The comparative analysis of numerical results presented in Table 1, leads to the conclusion that the most effective waveguide for the generated waves, is the one with flat sides (parameter $k=0$). Such a waveguide yields the greatest wave amplitude during propagation of a tsunami with the initial height of 2 meters (Table 1).

Table 1.

Coefficient k	Minimum wave amplitude	Maximum wave amplitude
- 150	- 88	+ 87
- 100	- 82	+ 113
- 50	- 91	+ 121
0	- 167	+ 184
50	- 110	+ 119
100	- 73	+ 45
150	- 106	+ 60

Numerical modeling of tsunami propagation along the real Pacific waveguide was carried out with the model tsunami source, which produced the initial two meters high tsunami wave. The 600x720 points computational grid included the Izu-Nanpo island chain southward of Japan (Fig. 13). The bottom relief was taken from Smith-Sandwell 2 arc minute Global digital bathymetry [4]. The initial tsunami source has the same profile as in previous computation experiments but its length is equal to the whole computational area width (600 grid steps). Looking at Figures 14(a-c) it is seen that wave energy is concentrated above the bottom ridge. Tsunami waves here are much higher than ones outside this natural waveguide. The maximum of tsunami height was detected at the Izu peninsula, where the bottom ridge comes out from the deep ocean onto a shelf.

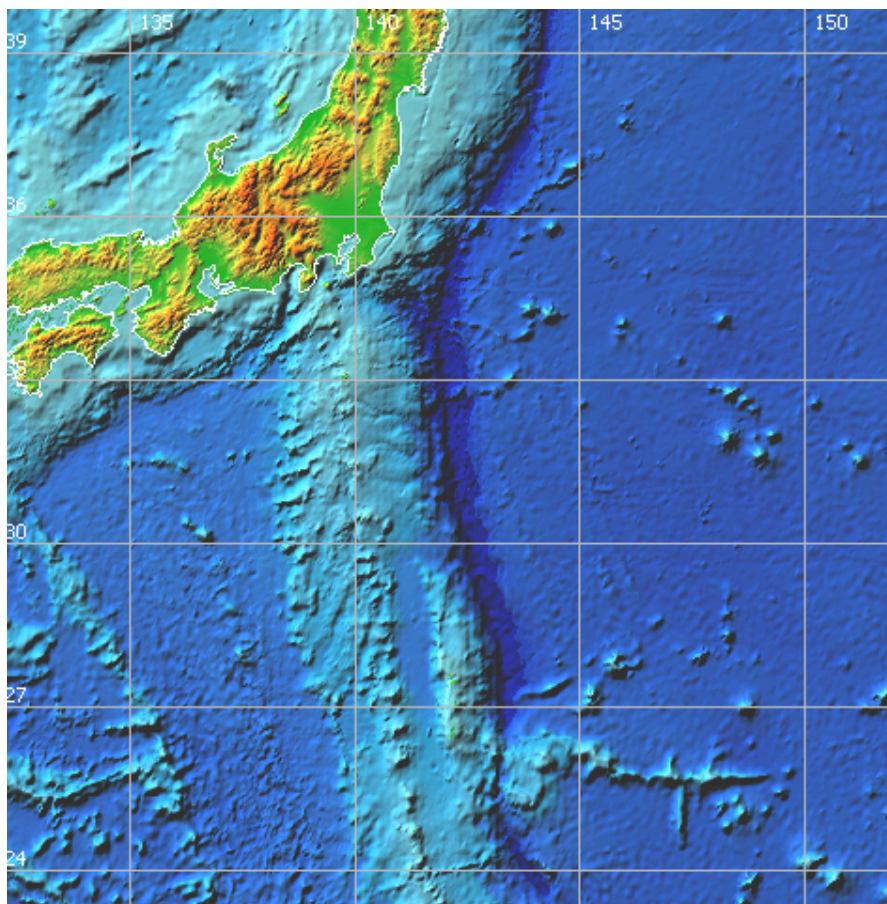


Fig. 13. The bottom relief in numerical computations of tsunami propagation along the Izu-Nanpo island chain

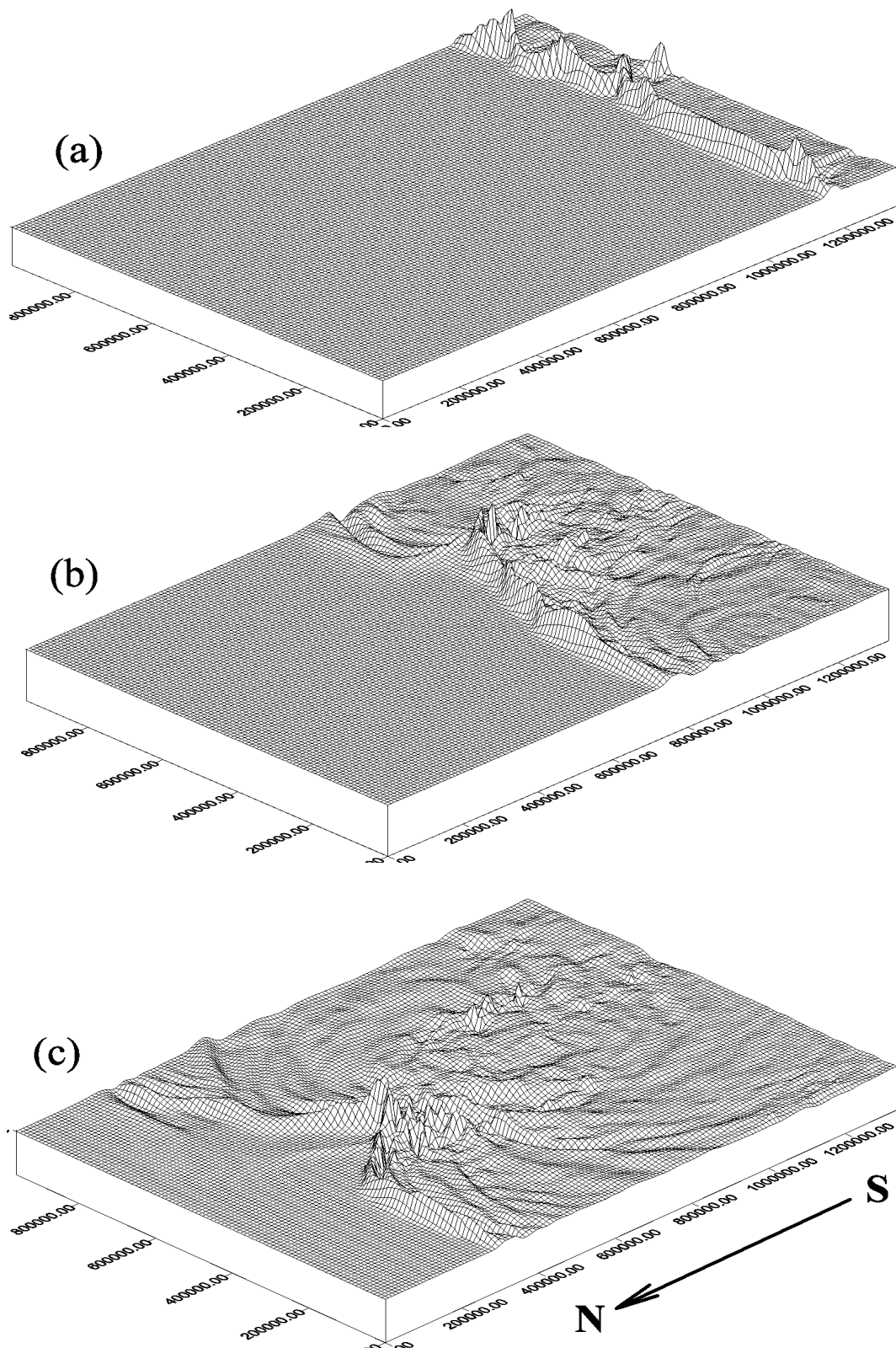


Fig. 14. Water surface during tsunami wave propagation above the Izu-Nanpo bottom ridge

Another example of the ocean bottom ridges influence to the tsunami propagation process can be found in another study [5]. In this paper some field data of tsunami 26 December 2004 and

results of numerical modeling of its global propagation are presented. Based on a comparative analysis of the maximum of the calculated amplitude in World Ocean (Fig. 15) and the World Ocean bathymetry (Fig. 16), it may be concluded that some bottom ridges (dash lines in Fig. 16) acted as tsunami waveguides. The travel-time charts of the tsunami of 26 December 2004 [5] also confirm the waveguide mode of tsunami propagation above some Pacific bottom ridges.

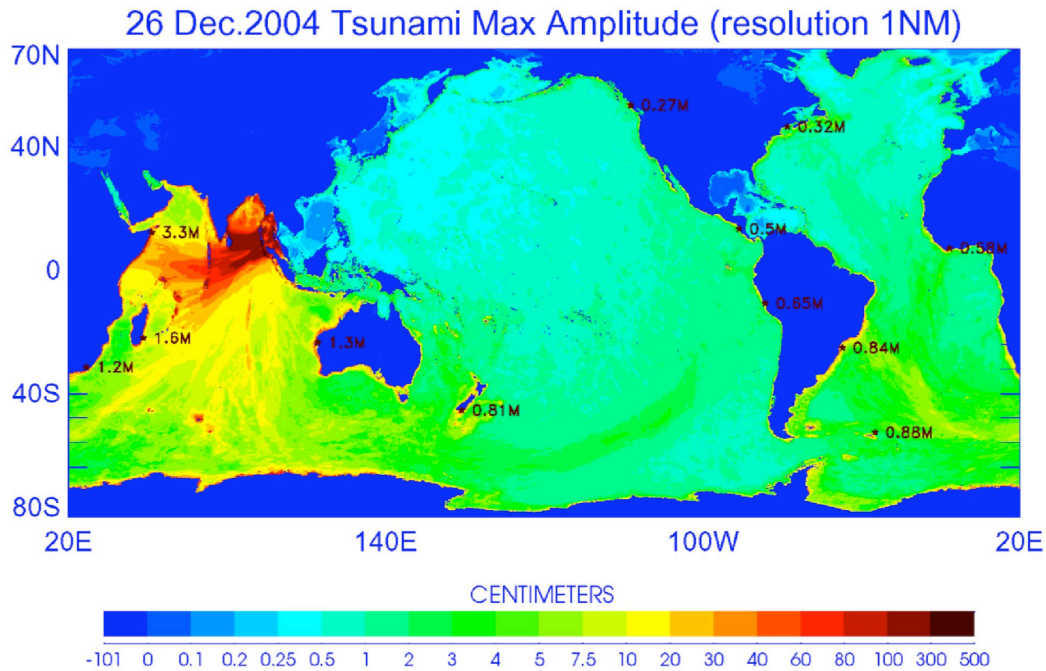


Fig. 15. Maximum of the calculated amplitude in World Ocean [5]

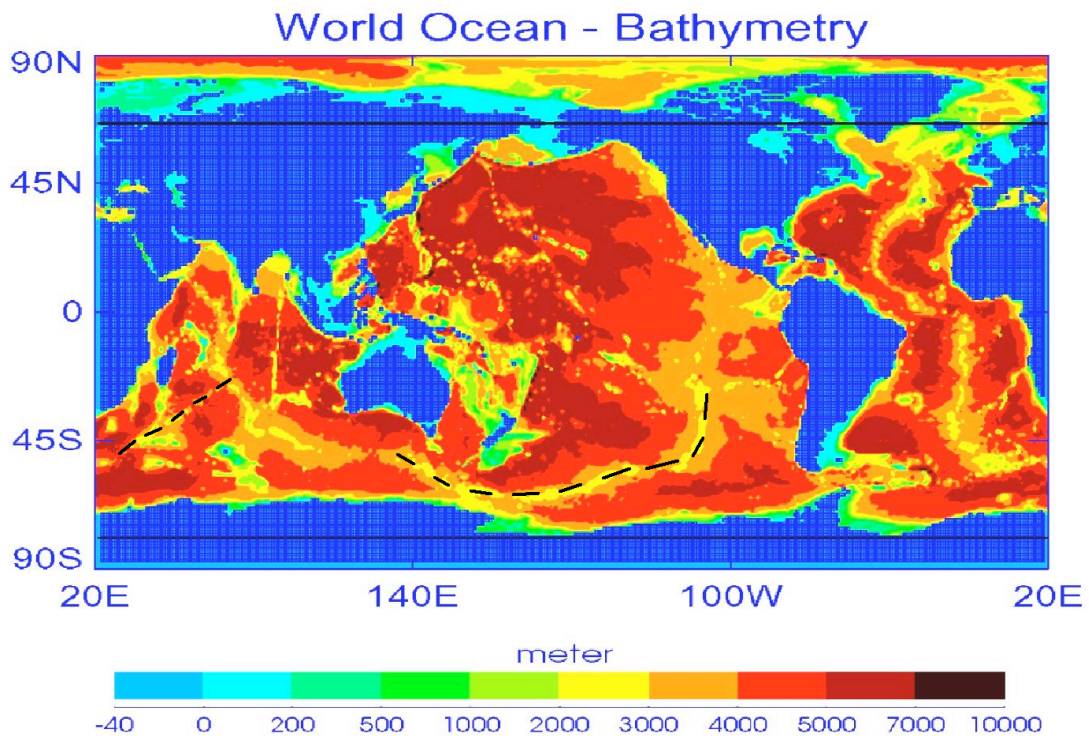


Fig. 16. Ocean bathymetry that was used for numerical modeling [5]

Acknowledgments

The work is supported by SBRAS Grant for Integration project No. 2006/113 and RFBR grants 07-05-13583, 08-07-00105.

References

1. Brekhovskikh, L.M., 1957, *Waves in stratified media* (in Russian) Moscow: USSR Academy of Sciences, 1957.
2. Elsgol'ts A.E., 1969, *Differential equations and a calculus of variations* (in Russian). Moscow, Nauka, 1969, 424p.
3. Titov, V.V., 1989, Numerical modeling of tsunami propagation by using variable grid. *Proceedings of the IUGG/IOC International Tsunami Symposium*, Computing center Siberian Division USSR Academy of Sciences, Novosibirsk, USSR, 1989, pp. 46-51.
4. Smith W.H.F. and Sandwell D. 1997. Global seafloor topography from satellite altimetry and ship depth soundings. *Science*. 277: 1956-1962.
5. Z. Kowalik, T. Logan, W. Knight and P. Whitmore, 2005. Numerical modeling of the global tsunami: Indonesian tsunami of 26 December 2004. *Science of Tsunami Hazards*, Vol. 23, No. 1, (2005), pp.40-56